

# Homology modeling, molecular dynamic simulation and docking studies of cyclin dependent kinase 1

Lei Zhang · Huawei Zhu · Qiang Wang · Hao Fang ·  
Wenfang Xu · Minyong Li

Received: 31 December 2009 / Accepted: 18 March 2010 / Published online: 26 April 2010  
© Springer-Verlag 2010

**Abstract** In order to develop promising cyclin dependent kinase 1 inhibitors, homology modeling, docking and molecular dynamic simulation techniques were applied to get insight into the functional and structural properties of cyclin dependent kinase 1 (CDK1). Since there is no reported CDK1 crystal structural data, the three dimensional structure of CDK1 was constructed based on homology modeling. An extensive dynamic simulation was also performed on a Flavopiridol-CDK1 complex for probing the binding pattern of Flavopiridol in the active site of CDK1. The binding modes of other inhibitors to CDK1 were also proposed by molecular docking. The structural requirement for developing more potent CDK1 inhibitors was obtained by the above-mentioned molecular simulations and pharmacophore modeling.

**Keywords** Cyclin-dependent kinase 1 (CDK1) · Docking · Homology modeling · Molecular dynamic simulation · Pharmacophore identification

## Introduction

Cyclin-dependent kinases (CDKs) are a family of serine/threonine kinases that are essential for cell cycle progres-

sion by activating host proteins through phosphorylation on serine or threonine using adenosine triphosphate (ATP) as a phosphate donor. The CDK-cyclin complexes drive cells from G1 into M phase through the restriction points to complete the cell cycle progression [1].

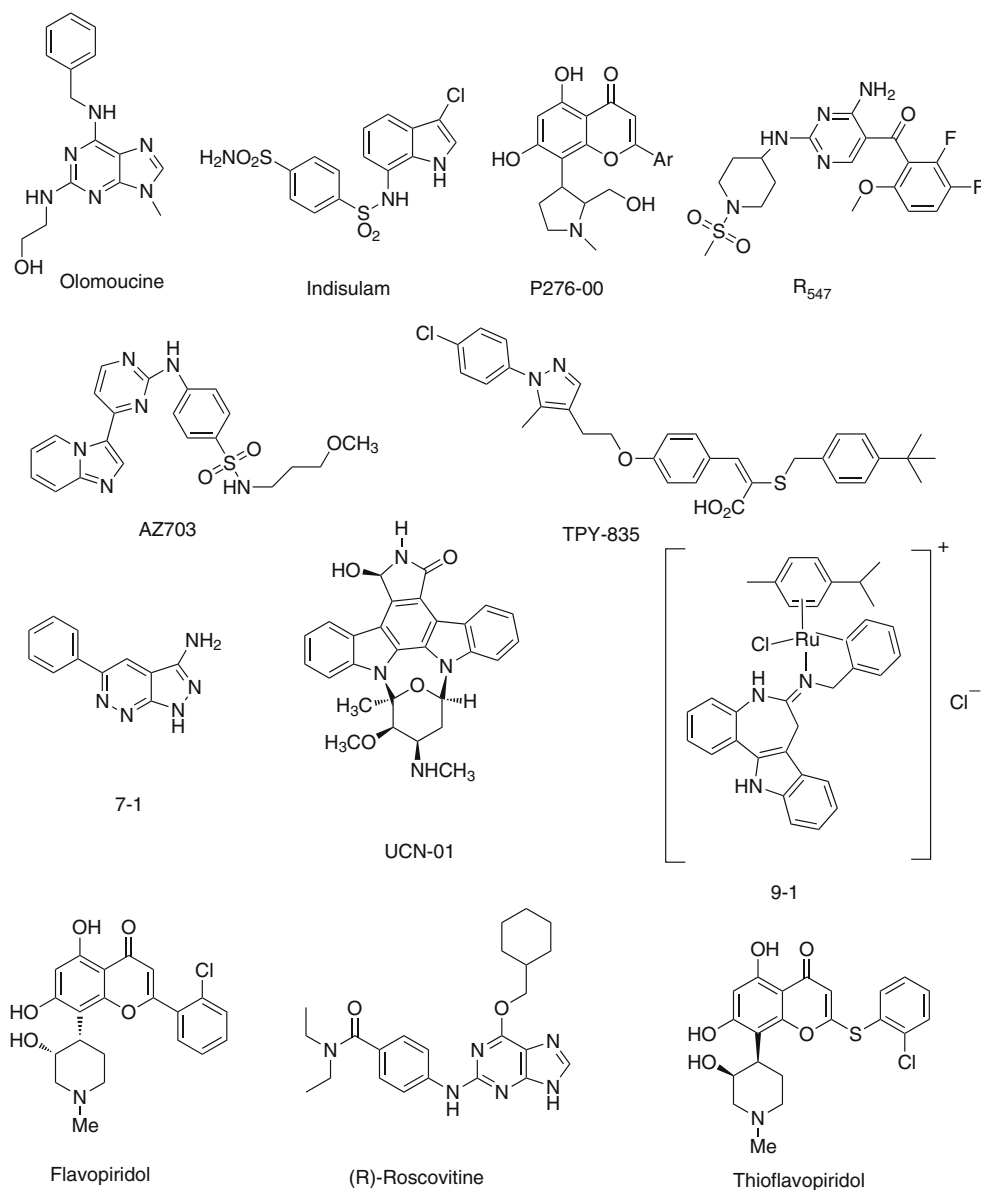
At present, 13 members of the CDK family have been reported, which are named from CDK1 to CDK13. Among these members, CDK1, CDK2, CDK4 and CDK6 regulate cell cycle directly, in the meanwhile CDK7 controls the cycle by activating other CDKs. In addition, CDK8, 9, 7 are transcription regulatory factors. Moreover, CDK2, CDK4, and CDK6 mediate G1 phase of cell cycle, whereas CDK2 and CDK1 regulates S and G2 phase, and M phase, respectively [2–6].

So far hundreds of CDK inhibitors (CDKIs) have been developed for anti-tumor proposes because the overproduction of CDKs has an intrinsic correlation with the pathogenesis of cancer [7]. Various structure-diverse molecule inhibitors, such as Olomoucine [8, 9], Indisulam [10], P276–00 [11], R547 [12], AZ703 [13], TYP–835 [14], 7–1 [15], UCN–01 [16–18] and 9–1 [19] (Fig. 1) exhibit good potential in the preclinical or clinical studies.

Focusing on the inhibition of CDK1 for cancer therapy, our group has developed fruitful inhibitors, for example, flavopiridol derivatives with interesting activities [20]. On the forthcoming chemical modification and optimization of CDKIs, we need an extensive understanding on the structural basis of CDK proteins. Therefore, in the current manuscript we would like to model the theoretical structure of CDK1 and simulate the interaction between CDK1 and its inhibitors by using computational approaches.

L. Zhang · H. Zhu · Q. Wang · H. Fang · W. Xu (✉) · M. Li (✉)  
Department of Medicinal Chemistry, School of Pharmacy,  
Shandong University,  
Jinan, Shandong 250012, China  
e-mail: xuwenf@sdu.edu.cn  
e-mail: mli@sdu.edu.cn

**Fig. 1** Structures of some CDK inhibitors of different categories



## Materials and methods

### Homology modeling

The sequence of human CDK1 was downloaded from NCBI protein data bank (Swiss-Prot entry: P06493). The crystal structures of human CDK2 (PDB entry: 3EZR), CDK5 (PDB entry: 1H4L), CDK6 (PDB entry: 1JOW), CDK7 (PDB entry: 1UA2), CDK4 (PDB entry: 2W9F) and CDK9 (PDB entry: 3BLH) as modeling templates were all derived from the Protein Data Bank.

The homology modeling was performed using the SYBYL 7.3 software running on a DELL Precision 360 workstation. The FUGUE program [21] was used to align these seven homology sequences and determine the

relationship between the sequence of CDK1 and other structures. The CDK1's 3D structure was constructed using the ORCHESTAR [22] module based on the crystal structure of the six homologous CDK proteins. The structure of structurally conserved regions (SCRs) which define the common tertiary folding pattern and the loops which connect the SCRs were constructed by turns. The final structure was verified by Phi/Psi and Profiles-3D analyses [23, 24].

### Molecular dynamic simulation

The molecular dynamic simulation was managed using the GROMACS 4.0 software (<http://www.gromacs.org>) [25–27]. The Flavopiridol-CDK1 complex was derived by

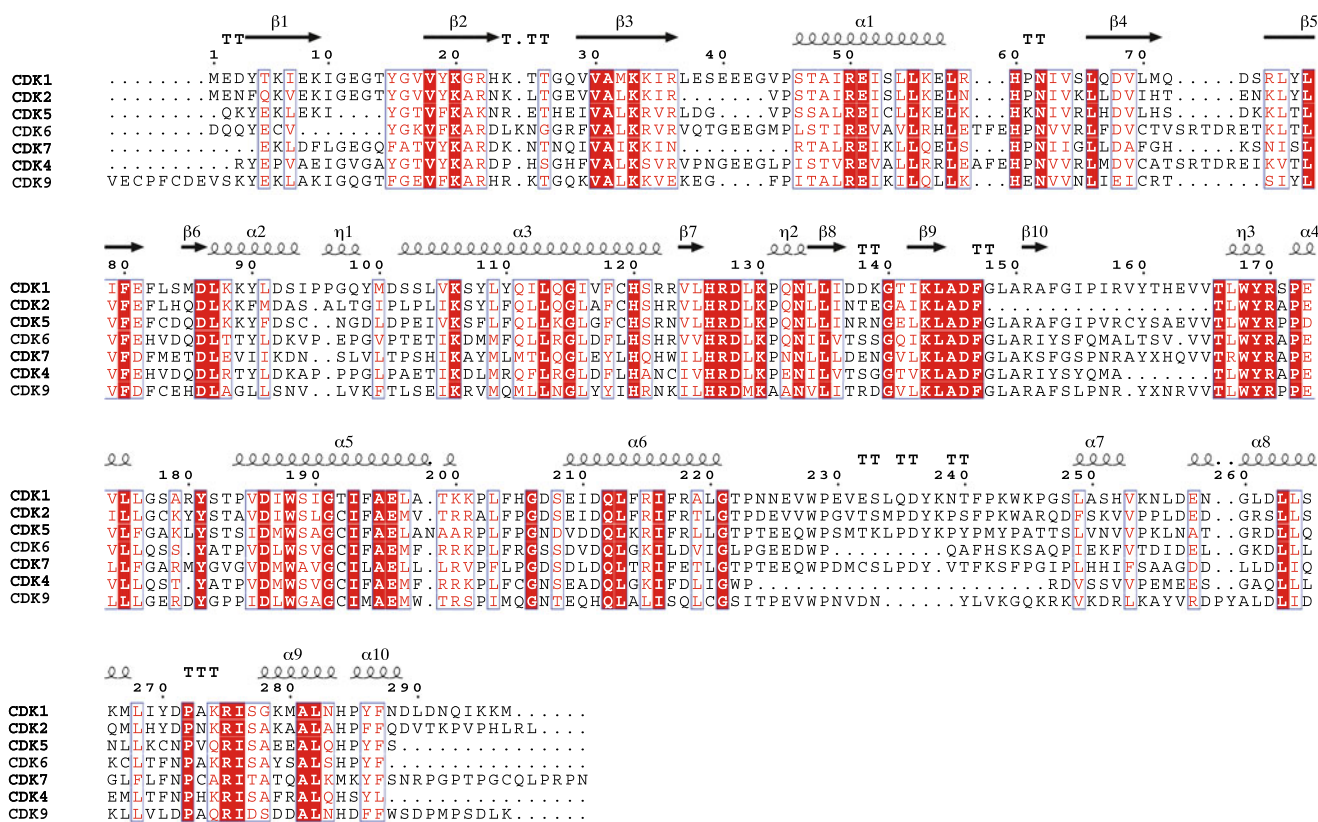


**Fig. 2** Sequence alignment of human CDK1 to the templates

docking Flavopiridol [28] to CDK1 model using FlexX2 docking program [29, 30]. The simulation was performed using a cubic cell geometry, and the default simple point charge (SPC) water was added to the box. Periodic boundary condition was applied, the distance between the grid box and the protein was set to 1.0 nm. Firstly, a steepest descents minimization for 500 steps was performed to remove bad *van der Waals* contacts. Then a 30 ps position-restrained simulation was performed by keeping the protein coordinates fixed, and making the water molecules soak into the macromolecule. The particle mesh Ewald (PME) [31] method was used for computing long-

range electrostatics. Finally, a 6 ns dynamic simulation was submitted at 310 K temperature and 1 bar pressure. The Berendsen temperature coupling and Berendsen pressure coupling (the coupling constants were both set to 0.1) were used to keep the system in a stable environment.

Probing the interaction of CDK1 and inhibitors

The molecular docking was used to determine the binding patterns of three representative CDK1 inhibitors, including R547, (R)-Roscovitine [32, 33] and Thioflavopiridol [34] (Fig. 1), around the active site of CDK1 by employing the

**Table 1** Analysis of template structures and the derived CDK1 model

|   | 3EZr   | 1H4l   | 1JOW   | 1UA2   | 2W9F   | 3BLH   | CDK1   |
|---|--------|--------|--------|--------|--------|--------|--------|
| Zscore                                  | 59.86  | 57.25  | 39.08  | 40.72  | 36.48  | 36.78  | –      |
| Verify score                            | 125.89 | 119.35 | 111.88 | 104.03 | 107.56 | 125.97 | 127.04 |
| Expected high score                     | 124.13 | 126.42 | 125.97 | 130.55 | 118.63 | 132.84 | 135.14 |
| Expected low score                      | 55.86  | 56.90  | 56.68  | 58.75  | 53.39  | 59.78  | 60.81  |
| Number of residues in core region       | 257    | 246    | 224    | 250    | 214    | 243    | 279    |
| Number of residues in allowed region    | 9      | 25     | 40     | 21     | 31     | 32     | 8      |
| Number of residues in disallowed region | 7      | 7      | 13     | 16     | 16     | 17     | 10     |

FlexX2 docking program in SYBYL 7.0 package. In the docking process, MMFF94 charges were assigned to both the protein and the inhibitors, maximum number of poses per ligand was set to 30 and other parameters were set as default. Moreover, a pharmacophore model of the CDK1's active site was also generated using HipHop algorithm [35] in Discovery Studio 2.5 package to look up the common features of CDK1 inhibitors.

## Results and discussion

### Verification of the constructed model

CDK1 shares a 64%, 44%, 56%, 46%, 44% and 41% sequence identity with CDK2, CDK4, CDK5, CDK6, CDK7 and CDK9, respectively (Fig. 2). This evidence reveals that these six homologous proteins are appropriate templates for building up the CDK1 model. The main chain root mean square deviation (RMSD) of the derived CDK1 homology model with CDK2, CDK4, CDK5, CDK6, CDK7 and CDK9 is 1.241, 1.337, 0.748, 0.967, 1.258 and 0.813 Å, respectively. These low RMSD values indicated a reasonable initial coordinate for further MM and MD calculations

The Zscore given by the FUGUE program showed that all six templates were suitable to be used ( $Zscore \geq 6$ ) (Table 1). The Phi/Psi analysis of the model exhibits 279 residues in the core region, 8 in the allowed region and 10 at the disallowed position, respectively (Fig. 3A). These results disclose that the derived model is of high quality for further study. The verify score of the model is 127.04 in the

**Fig. 3** (a) The Ramachandran plot of the constructed CDK1 model. (b) Secondary structure of the constructed CDK1 model colored by verify score, blue: high score; red: low score

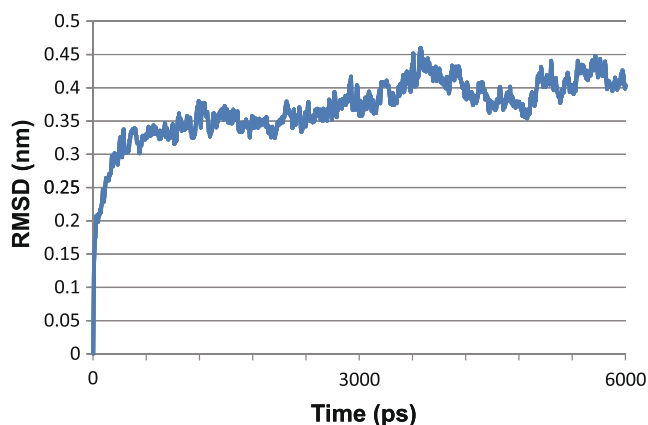
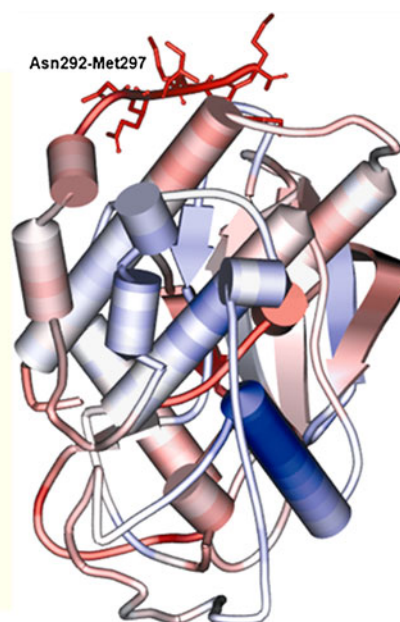
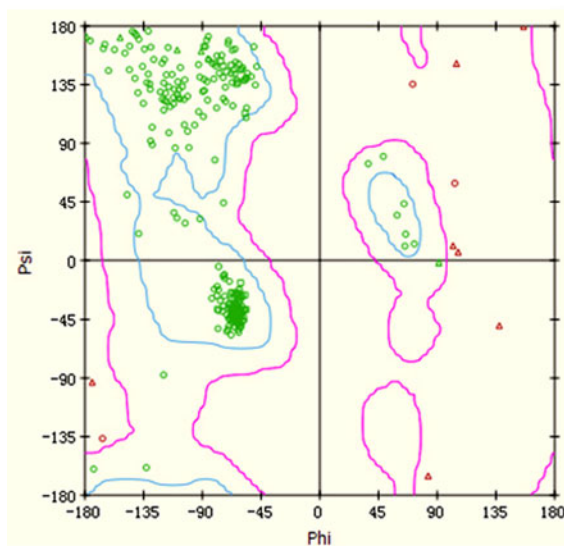


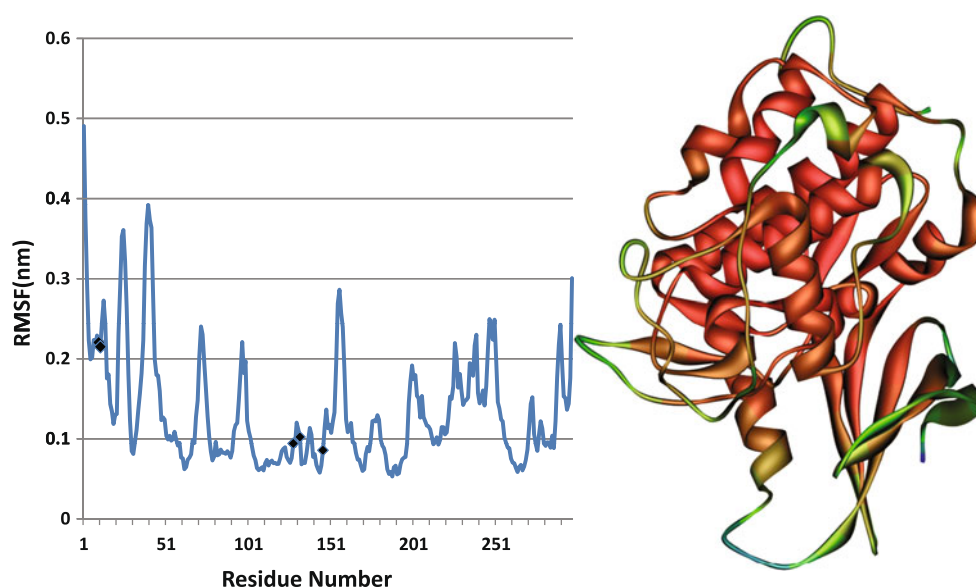
**Fig. 4** The RMSD plot of the protein during the dynamic simulation

Profiles\_3D analysis compared to verify expected high score (135.14) and verify expected low score (60.81). The scored structure showed that the last 6 residues in the C terminal may have low verify score for negative contribution to the quality of the model (Fig. 3B). The results of all these evaluations suggest a high quality homology model for CDK1 again.

### Molecular dynamic simulation

The root mean square deviation (RMSD) value of the complex tends to be convergent with fluctuations around 3.5 Å after 2.0 ns of simulation. This evidence clearly indicates that the whole system is stable and has been equilibrated (Fig. 4). The root mean square fluctuation (RMSF) plot shows that residues in the N terminal have the

**Fig. 5** Left: The root mean square fluctuation of CDK1 during the 6 ns simulation. Residues in the active site are represented with black points. Right: The structure of CDK1 which was colored by RMSF value of the residues, as the value increasing the surface was changed from red to green and to blue



biggest magnitude of movement, the C terminal and some flexible loops are also prone to fluctuation (Fig. 5).

Multiple H-bond interactions were found in Ile10, Gly11, Asp128, Gln132 and Asp146 by analyzing the simulated complex coordinate (Fig. 6). The distances of corresponding atom pairs were summarized in Table 2. It is obvious that Asp146 can function as an H-bond donor by forming duplicate H-bond interactions with N27 and O5 of Flavopiridol. Asp128 can also play a donor role by supporting hydrogen bonding to N27. Gln132 may accept proton from O4. Ile10 and Gly11 can form H-bond interactions with O2 and O3, respectively.

The contribution of water molecules were observed to the binding of the ligand-receptor complex (Fig. 7). Three water molecules, water2780, 5194 and 6875 bridged the gap between Flavopiridol and residues Lys130 and Gln132.

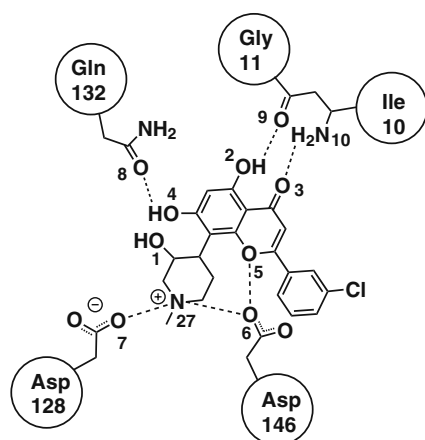


**Fig. 6** 2D representation of H-bond interaction between Flavopiridol and the surrounding residues

The RMSD values show that these water molecules possess tiny extent of movement during the 6 ns simulation procedure (Fig. 8). Thus, these three water molecules can surrogate an intermolecular H-bond network to stabilize the Flavopiridol-CKD1 interaction. Water2780, functioning as an acceptor, is able to form two H-bonds with O4 of Flavopiridol and NH<sub>2</sub> of Gln132, and at the same time, functioning as an acceptor, forms a H-bond with CO of GLN132. Water5194 has the ability to form three H-bonds with O2, O3 of Flavopiridol and NH<sub>2</sub> of Gln132, respectively. Water 6875, as an acceptor, can form three H-bonds with O1, O4 of Flavopiridol and NH<sub>3</sub> of Lys130, respectively, and as a donor, can form H-bond with CO of Gln132.

#### Docking analysis

Three potent CDK1 inhibitors were docked into the active site of CDK1 for probing the binding modes of the ligand-target complexes. There is a big hydrophobic pocket around the active site of CDK1 as revealed in Fig. 9. This

**Table 2** The distance between polar atoms of Flavopiridol and corresponding residue atoms

| Atom pairs                   | Distance(Å) |
|------------------------------|-------------|
| O2(Flavopiridol)–O9(Ile10)   | 4.1±1.0     |
| O3(Flavopiridol)–O10(Gly11)  | 4.0±1.0     |
| O4(Flavopiridol)–O8(Gln132)  | 3.8±1.2     |
| O5(Flavopiridol)–O6(Asp146)  | 3.6±1.1     |
| N27(Flavopiridol)–O6(Asp146) | 3.7±0.8     |
| N27(Flavopiridol)–O7(Asp128) | 3.1±0.5     |

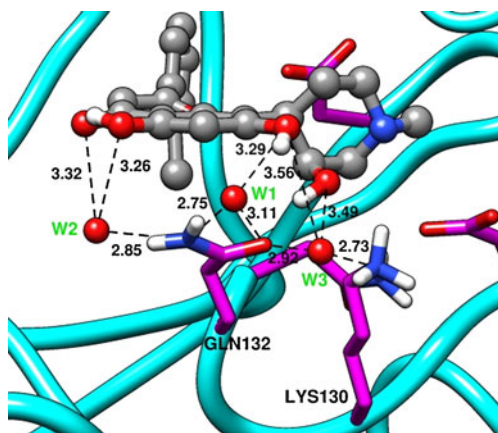


**Fig. 7** Binding patterns of waters in the active site of CDK1. W1: water2780, W2: water5194, W3: water6875. The structure was extracted from the simulation at 4050 ps. The picture was made by the UCSF chimera software [36]

lipophilic pocket is divided into two parts, one is big, and the other is relatively small. There are some polar residues (such as Ile10, Glu12, Gln132, and Asn133) lined in the opening of the cavity by forming strong H-bond interaction with ligands located in the pocket. The hydrophobic side chains of compound R547 (a) and Thioflavopiridol (b) extended to the two different pockets, respectively. Thus,

the hydrophobic interactions make important contributions to the binding of the inhibitors to the active site. H-bonding interactions formed between the inhibitors and the core residues were signed in Fig. 8. It is obvious that H-bond interaction is also very important in the ligand receptor binding for the three inhibitor molecules. In order to form strong H-bond interactions the cyclohexane group of (R)-Roscovitine stretched out of the cavity (c) which is different from other molecules.

A pharmacophore model of the constructed CDK1 active site was also generated to verify and compare the docking results (Fig. 10). Similar information was derived from the pharmacophore hypothesis with the docking studies. In the opening of the pocket, Ile10 provides H-bond donor, Glu12 and Lys130 provide H-bond acceptors. There are both H-bond donor and acceptor in Asp146 which locates inside the pocket. There is also hydrophobic feature inside the pocket. It must be noted that Leu83 on the edge of the pocket is a potential H-bond interaction site which was not discovered in the docking analysis.

For designing more potent CDK1 inhibitors, firstly and most importantly, multiple H-bond donors and receptors should be kept in the inhibitors' structure, because the hydrogen bonding is proved to play so important a role in the ligand-receptor interactions. For designing Flavopiridol derivatives, the side chain stretched to the bigger

**Fig. 8** RMSD values of the water molecules during the 6 ns simulation. The RMSD plot of water 1671 was used to compare with the above three waters

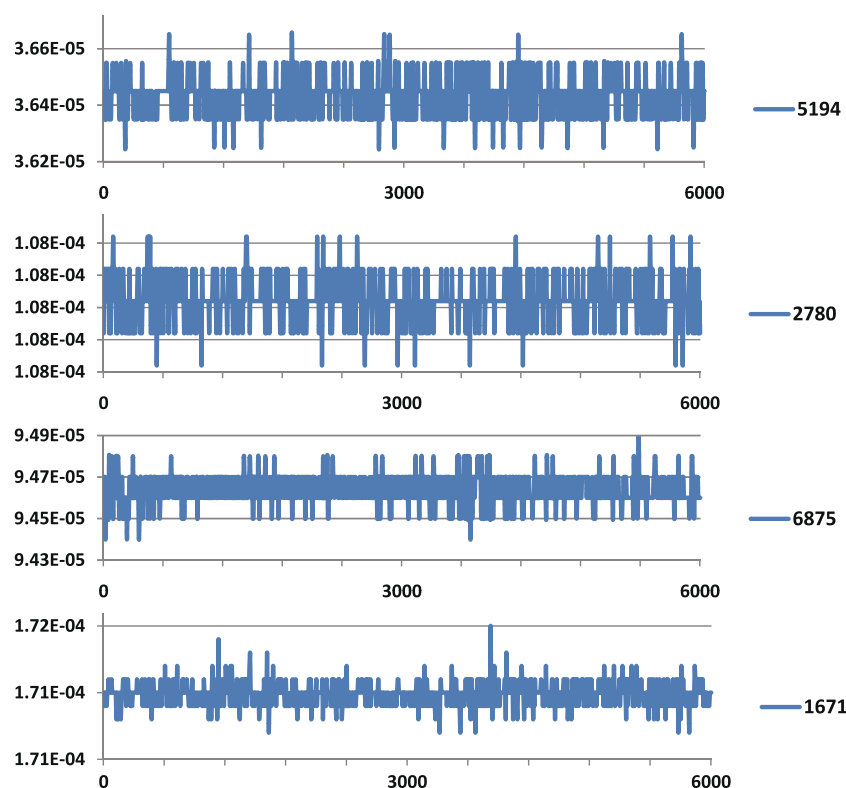
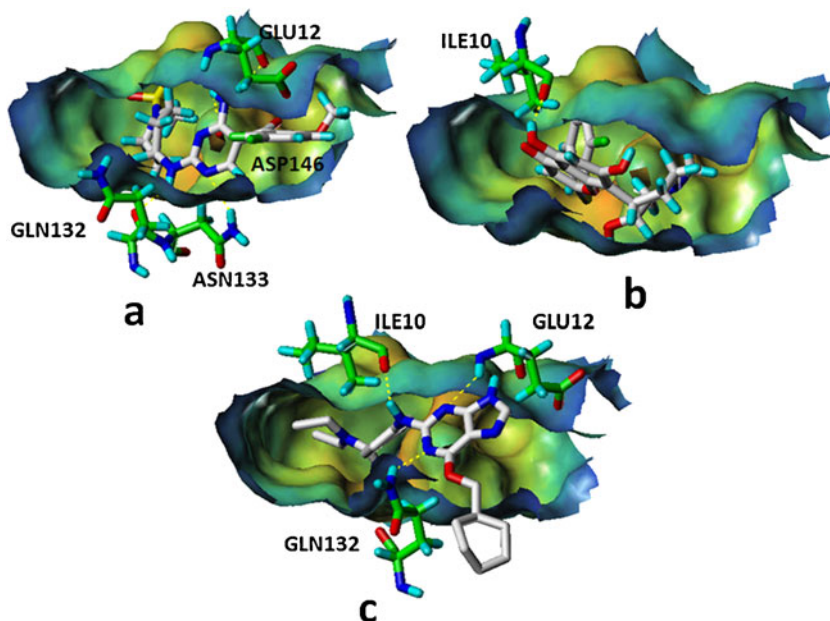


**Fig. 9** Binding patterns of inhibitors in the active site of CDK1, (a) R547, (b) Thioflavopiridol, (c) (R)-Roscovitine. H-bonds are represented as dot lines. The molecular surface of the active site was created by MOLCAD in Sybyl7.0, the Cavity Depth surface property was represented



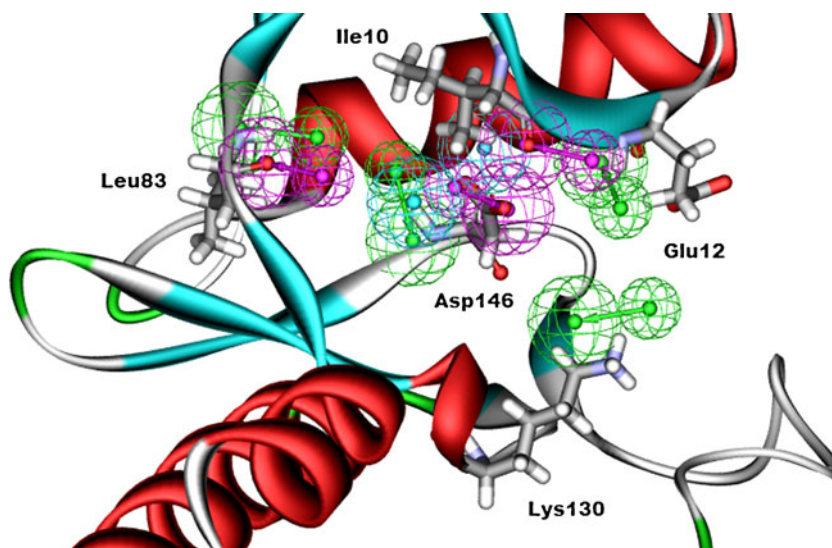
pocket should be prolonged with hydrophobic groups (fixing to the hydrophobic pocket) ended with polar atoms (binding to Leu83). Furthermore, some oxygen atoms in the molecular scaffold should be replaced by nitrogen and sulphur atoms for improving H-bond binding in the opening of the pocket.

## Conclusions

In order to improve our efficiency and rationality for developing potent CDK1 inhibitors, the 3D homology

structure of CDK1 was constructed. The modeling structure was verified to be of good quality and thus being used for the subsequent analysis. Molecular dynamic simulation was performed to gain deep insight on the structural property of the model and binding details of the Flavopiridol-CDK1 complex. Docking and pharmacophore modeling methods were also applied for further study interaction between other inhibitors and core residues to provide the structural requirement of the inhibitors for binding to CDK1. Finally, such methods for improving the binding were concluded and these ideas will be applied and verified in our further work.

**Fig. 10** The pharmacophore model of CDK1 active site. The features are H-bond acceptors (green), H-bond donors (magenta) and hydrophobic centers (cyan). The core residues are Ile10, Glu12, Leu83, Lys130, and Asp146, respectively



**Acknowledgments** This work was supported by Project of Science and Technology Research in Shandong Province (2008GG10002010) and Independent Innovation Foundation of Shandong University, IIFSDU (2009TS111). We also acknowledge Accelrys Inc. for providing the Discovery Studio 2.5 package.

## References

1. Lees E (1995) *Curr Opin Cell Biol* 7:773–780
2. Morgan DO (1997) *Annu Rev Cell Dev Bi* 13:261–291
3. Jeffrey PD, Russo AA, Polyak K, Gibbs E, Hurwitz J, Massague J, Pavletich NP (1995) *Nature* 376:313–320
4. Dunphy WG (1994) *Trends Cell Biol* 4:202–207
5. Hoffman I, Karsenti E (1994) *J Cell Sci* 18:75–79
6. Hochegger H, Takeda S, Hunt T (2008) *Nat Rev Mol Cell Bio* 9:910–U926
7. Knockaert M, Greengard P, Meijer L (2002) *Trends Pharmacol Sci* 23:417–425
8. Villerbu N, Gaben AM, Redeuilh G, Mester J (2002) *Int J Cancer* 97:761–769
9. Havlicek L, Hanus J, Vesely J, Leclerc S, Meijer L, Shaw G, Strnad M (1997) *J Med Chem* 40:408–412
10. Moon MJ, Lee SK, Lee JW, Song WK, Kim SW, Kim JI, Cho C, Choi SJ, Kim YC (2006) *Bioorg Med Chem* 14:237–246
11. Joshi KS, Rathos MJ, Joshi RD, Sivakumar M, Mascarenhas M, Kamble S, Lal B, Sharma S (2007) *Mol Cancer Ther* 6:918–925
12. DePinto W, Chu XJ, Yin XF, Smith M, Packman K, Goelzer P, Lovey A, Chen YS, Qian H, Hamid R, Xiang Q, Tovar C, Blain R, Nevins T, Higgins B, Luistro L, Kolinsky K, Felix B, Hussain S, Heimbrook D (2006) *Mol Cancer Ther* 5:2644–2658
13. Byth KF, Geh C, Forder CL, Oakes SE, Thomas AP (2006) *Mol Cancer Ther* 5:655–664
14. Aoyagi Y, Masuko N, Ohkubo S, Kitade M, Nagai K, Okazaki S, Wierzba K, Terada T, Sugimoto Y, Yamada Y (2005) *Cancer Sci* 96:614–619
15. Brana MF, Cacho M, Garcia ML, Mayoral EP, Lopez B, de Pascual-Teresa B, Ramos A, Acero N, Llinares F, Munoz-Mingarro D, Lozach O, Meijer L (2005) *J Med Chem* 48:6843–6854
16. Sielecki TM, Boylan JF, Benfield PA, Trainor GL (2000) *J Med Chem* 43:1–18
17. Dasmahapatra GP, Didolkar P, Alley MC, Ghosh S, Sausville EA, Roy KK (2004) *Clin Cancer Res* 10:5242–5252
18. Grosios K (2001) *Curr Opin Invest Drugs* 2:287–297
19. Schmid WF, John RO, Muhlgassner G, Heffeter P, Jakupec MA, Galanski M, Berger W, Arion VB, Keppler BK (2007) *J Med Chem* 50:6343–6355
20. Li YL, Fang H, Xu WF, Wang BH (2008) *Chin Chem Lett* 19:541–543
21. Shi JY, Blundell TL, Mizuguchi K (2001) *J Mol Biol* 310:243–257
22. Blundell TL, Elliott G, Gardner SP, Hubbard T, Islam S, Johnson M, Mantafounis D, Murray-Rust P, Overington J, Pitts JE, Sali A, Sibanda BL, Singh J, Sternberg MJE, Sutcliffe MJ, Thornton JM, Travers P (1989) *Phil Trans R Soc Lond B* 324:447–460
23. Lüthy R, McLachlan AD, David E (1991) *Proteins* 10:229–239
24. Lüthy R, Bowie JU, Eisenberg D (1992) *Nature* 356:83–85
25. Berendsen HJC, van der Spoel D, van Drunen R (1995) *Comput Phys Commun Package* 91:43–56
26. Lindahl E, Hess B, van der Spoel D (2001) *J Mol Model* 7:306–317
27. Van der Spoel D, Lindahl E, Hess B, Groenhof G, Mark AE, Berendsen HJC (2005) *J Comput Chem* 26:1701–1718
28. Brusselbach S, Nettelbeck DM, Sedlacek HH, Muller R (1998) *Int J Cancer* 77:146–152
29. Rarey M, Kramer B, Lengauer T, Klebe G (1996) *J Mol Biol* 261:470–489
30. Rarey M, Kramer B, Lengauer T (1997) *J Comput Aided Mol Des* 11:369–384
31. Darden T, York D, Pedersen L (1993) *J Chem Phys* 98:10089–10092
32. McClue SJ, Blake D, Clarke R, Cowan A, Cummings L, Fischer PM, MacKenzie M, Melville J, Stewart K, Wang SD, Zhelev N, Zheleva D, Lane DP (2002) *Int J Cancer* 102:463–468
33. Gherardi D, D’Agati V, Chu THT, Barnett A, Gianella-Borradori A, Gelman IH, Nelson PJ (2004) *J Am Soc Nephrol* 15:1212–1222
34. Kim KS, Sack JS, Tokarski JS, Qian LG, Chao ST, Leith L, Kelly YF, Misra RN, Hunt JT, Kimball SD, Humphreys WG, Wautlet BS, Mulheron JG, Webster KR (2000) *J Med Chem* 43:4126–4134
35. Clement OA, Mehl AT (2000) HipHop: pharmacophores based on multiple common-feature alignments. In: Güner OF (ed) *Pharmacophore Perception. Development & Use In Drug Design*. International University Line, La Jolla, pp 69–84
36. Pettersen EF, Goddard TD, Huang CC, Couch GS, Greenblatt DM, Meng EC, Ferrin TE (2004) *J Comput Chem* 25:1605–1612